ROLE OF AUTOMATED MINERAL ANALYSIS IN THE CHARACTERISATION OF MINING-RELATED CONTAMINATED LAND

DUNCAN PIRRIE[1], GAVYN K. ROLLINSON[2] AND MATTHEW R. POWER[3]

Pirrie, D., Rollinson, G.K. and Power, M.R. 2009. Role of automated mineral analysis in the characterisation of mining-related contaminated land. *Geoscience in South-West England*, **12**, 162-170.

The characterisation of soils or sediments contaminated as a result of historical metal mining activity is commonly carried out either by analysing the bulk geochemistry, or through methods which are aimed at assessing the biologically available component of the contaminant, such as physiologically based extraction techniques (P-BET tests). However, an understanding of the mineralogy or phase composition of particulate contaminants is critical in understanding both the long term geochemical stability of the contaminated sediments/soils, and also the development of potential remediation strategies, where required. Providing statistically robust mineralogical datasets based on traditional techniques is commonly difficult. However, modern advanced automated SEM-EDS mineral analysis systems have considerable potential in the characterisation of contaminated soils/sediments.

Six sediment samples collected from a single shallow core, recovered from the Hayle Estuary, Cornwall, UK have been analysed using QEMSCAN® automated SEM-EDS analysis. This estuary was significantly contaminated as a result of the release of mine waste tailings, principally from tin, copper, arsenic and zinc mining operations particularly between the 1850s and the 1890s. The samples analysed contain between ~2 and 6% sulphide and other ore minerals. In addition, there are significant depth-related changes in the overall bulk mineralogy of the samples reflecting the change in sediment supply to the estuary. For some elements (e.g. Sn) there is a reasonable correspondence between the measured bulk geochemistry of the sediments, with calculated elemental concentrations based on the measured mineralogical data. In this case study, Sn is probably occurring in cassiterite and possibly Sn slags and is relatively geochemically immobile. Other elements, such as arsenic and zinc show greater variance between the calculated elemental concentrations and the measured bulk chemistry, although the down-core trends are consistent. This can be interpreted as reflecting the increased geochemical mobility of these elements, resulting in them being under-reported. The data from automated mineralogy are however, extremely relevant in the assessment of metal contaminated land.

[1]Helford Geoscience LLP, Menallack Farm, Penryn, Cornwall, TR10 9BP, U.K.
[2]Camborne School of Mines, College of Engineering, Mathematics and Physical Sciences, University of Exeter, Cornwall Campus, Penryn, Cornwall, TR10 9EZ, U.K.
[3]36 Cherry Tree Lane, Colwyn Bay, North Wales, U.K.
(E-mail: dpirrie@helfordgeoscience.co.uk).

Keywords: Contaminated land, automated mineralogy, QEMSCAN®, Cornwall.

INTRODUCTION

A wide range of geochemical techniques can be applied during the site investigation of areas of metal contaminated land. Geochemical techniques alone are a valid approach in areas where the likely contaminant streams are aqueous or liquid chemical phases introduced as a result of human activity. However, in areas contaminated by historic metal mining, particulate contaminants may contribute significantly to the overall metal budget (e.g. Göktepe, 2005). The potential for the release of contaminants from these particulate wastes will depend on their mineralogy and the chemistry of the weathering environment they are exposed to (e.g. Isaure *et al.*, 2005). Bulk geochemical analyses will provide data on the total concentration of possible contaminant elements present, but will not provide sufficient data to assess the likely stability or bioavailability of those contaminants. In such cases mineralogical and petrographical data are also required. Mineral phases present within a metal mining contaminated soil or sediment might include grains of the original ore or gangue minerals, man-made secondary materials such as slags, and also secondary diagenetic phases formed as a result of alteration of the original waste materials or precipitated from metal-rich fluids (e.g. AMD). However, providing statistically robust mineralogical data for such soils and sediments may be problematic. In this paper mineralogical data collected using automated scanning electron microscopy with linked energy dispersive X-ray analysis (SEM-EDS) using QEMSCAN® technology, is presented for sediment samples collected from the Hayle Estuary, Cornwall, UK. The Hayle Estuary was extensively contaminated by waste from predominantly copper and tin mining, and subsequent mineral processing (e.g. Rollinson *et al.*, 2007). This study shows how automated mineralogy can provide robust data sets that can be used to evaluate mineral stability and potential bioavailability.

MINERALOGICAL AND GEOCHEMICAL TECHNIQUES IN THE CHARACTERISATION OF METAL-MINING WASTE STREAMS

Traditional geochemical and mineralogical techniques

In most countries, the legislative framework relating to the identification and treatment of contaminated land is based on the measurement of the samples geochemistry, and an assessment of the likely bioavailability and toxicity of the contaminant phases (e.g. Environment Agency, 2009). Legislation may either be based on the definition of trigger values - an absolute measured abundance of a particular element, above which site remediation is required, or may be based on a risk based approach, with the identification of the source-pathway-receptor models, and an understanding of the bioavailability and ecotoxicity of the elements being assessed (e.g. Luo *et al.*, 2009; Environment Agency 2009). Geochemical methods can either attempt to measure the total concentration of the elements of interest in a sample or may, through leachate experiments, attempt to measure the proportion of the contaminant phase that it likely to be bioavailable. Bulk geochemical techniques that are widely used include ICP-MS or ICP-OES, AAS or XRF. For ICP-MS, ICP-OES, AAS and in some cases, XRF analysis, the sample needs to be in solution prior to analysis, whilst traditional XRF analysis is based on either a pressed powder pellet or a fused bead. Geochemical techniques such as XRF or ICP-MS are advantageous in that they are relatively rapid, low cost and provide quantitative data with documented accuracy and precision. The limitation of such techniques, is simply that this is a bulk measure of the sample chemistry, and there is no understanding of the apportionment of the measured elements, to specific phases, within the sample. For example, in an area contaminated by the release of wastes from copper mining, a contaminated soil may contain: (a) grains of the ore minerals as either liberated, but unrecovered grains, or as grains of ore locked with other minerals (e.g. chalcopyrite, bornite, covellite etc); (b) secondary alteration phases derived from the surface weathering of the ore minerals (e.g. the copper chloride mineral atacamite); (c) if the ores have been smelted on site, then Cu may also occur within smelt waste products (slags). Bulk chemical analysis will not differentiate between these different phases, but the apportionment of the element of interest, in this case copper, is extremely important, as this will control the likely mobility and therefore bioavailability of the contaminant.

Consequently, in many studies of contaminated land, leachate experiments are carried out to try to assess what the bioavailable fraction of the contaminant phase of interest is. This is particularly common in for example, the analysis of the availability of arsenic or lead, where the physiologically-based extraction test (P-BET) test is commonly used (e.g. Bosso *et al.*, 2008; Intawongse and Dean, 2008). This procedure is intended to mimic the likely chemical reactions that an ingested particle would be subjected to during digestion. Once again, the reactivity, or solubility of the arsenic or lead-bearing particles, will depend upon the mineralogy or phase composition of that particle along with its size and texture. For example, a grain of arsenopyrite is far less soluble than a grain of arsenolite (Power *et al.*, 2009; Environment Agency, 2009).

In recent years, environmental mineralogy has become an important area of research within applied mineralogy, particularly with regard to sites contaminated as a result of mining and mineral processing (e.g. Rosado *et al.*, 2008). In essence, environmental mineralogy aims to understand mineral reactions in the near surface environment. A wide range of analytical approaches are used, including traditional transmitted and reflected light microscopy; X-Ray Diffraction (XRD); Scanning and transmission electron microscopy (SEM and TEM); electron microprobe analysis (EMPA); Raman microscopy etc (e.g. Isaure *et al.*, 2005; Bosso *et al.*, 2008). Commonly a combination of techniques is required to characterise the mineral phases (both opaque and translucent) and man-made particulates, present in a mine-waste contaminated site. Traditional microscopic techniques and manual scanning electron microscopy are very time consuming, particularly because in most sites contaminated by mining post the 1850s, the released particulate contaminants are predominantly in the <63 μm size fraction (and commonly occurring in the <20 μm size fraction). Bulk analytical techniques such as XRD are more rapid, and using quantitative techniques such as Rietveldt Analysis, can provide bulk modal mineralogy with detection limits of ~1-3%. However, XRD data do not provide textural, particle size or mineral association data that are derived from microscopy, although there have been recent advances in the development of micro-X-ray diffraction techniques that allow *in situ* analysis, with detection limits of 5±2% (Nel *et al.*, 2006).

Automated mineralogy

In the global mining industry, mineral process engineers are routinely using automated mineralogy to both (a) understand the ores that are the feed to their operations and also (b) to assess the recovery performance of mineral processing circuits by examining both the concentrates and the tails (e.g. Pascoe *et al*,. 2007; Benedictus *et al.*, 2008; Anderson *et al.*, 2009). Two automated mineralogy systems, both based on scanning electron microscopy, are in wide usage; QEMSCAN® and MLA. The last generation of QEMSCAN® systems are based on a Carl Zeiss EVO50 scanning electron microscope, with up to 4 light element Bruker SDD X-Ray detectors, along with the proprietary iExplorer® (comprising both iMeasure® and iDiscover®) software packages, that are used to both run the measurement and also process the resultant data files. Minerals and chemical compounds are identified using this system through the extremely rapid acquisition of ED X-Ray spectra on a pixel by pixel basis (see below). The mineral liberation analyser (MLA), is based on a FEI SEM platform, with typically 1 or 2 EDS detectors. The system identifies particles of interest based on the backscatter electron coefficient, and then acquires EDS spectra of BSE segmented regions of the particle. Although automated mineralogy is very widely utilised in the mining and mineral processing industry, there have been relatively limited published articles exploring the application of this technology in other areas, other than in forensic science (Pirrie *et al.*, 2004; Pirrie *et al.*, 2009), archaeology (Hardy *et al.*, 2006; Hardy and Rollinson, 2009) and aerosol particulates (Martin *et al.*, 2008). Recently, several studies relating to mine waste contamination have utilised QEMSCAN® technology (Camm *et al.*, 2003; Pirrie *et al.*, 2003; Power *et al.*, 2009).

There are several advantages in the use of automated mineralogy for the characterisation of mine-waste contaminated sites. (1) Translucent, opaque and man-made phases are all measured at the same time, providing the bulk modal mineralogy of the sample based on the measurement of typically 1000s of grains mapped by EDS analysis at anything down to a 0.5 μm beam stepping interval. Consequently the modal mineralogy is both statistically robust and reproducible (*cf.* Pirrie *et al.*, 2009). (2) Data on mineral associations, liberation characteristics, textures and particle and grain size are automatically captured along with the bulk mineralogy; these data can aid the interpretation of the likely source of the contaminants, and can also be used to assess their degree of alteration. (3) The sample analysis is operator independent during the measurement of the sample and very rapid, with typically greater than 1000 mineral grains at low concentration analysed per hour. However, the drawbacks to automated SEM-EDS analysis are that: (a) mineral polymorphs and phases with very similar chemistries cannot be distinguished from one another; (b) if contaminant phases are present absorbed or adsorbed onto the surface of other mineral grains, then they would not be identified; (c) as with any SEM-EDS analysis system most organic contaminants cannot be measured.

In this paper we provide a case study on the use of automated SEM-EDS analysis using QEMSCAN® technology on mine waste contaminated sediments from the Hayle Estuary, Cornwall, UK, and review the potential use of such data in the management of land and sediments contaminated as a result of metal mining.

Samples selected for analysis

The Hayle Estuary, Cornwall, UK, is today an important nature reserve, but historically received very significant quantities of particulate mining and mineral processing waste from copper, tin, zinc and arsenic workings in the estuary catchment area (Pirrie *et al.*, 1999; Rollinson *et al.*, 2007) (Figure 1). The geochemistry of both shallow (*c.* up to 1 m) cores recovered from the intertidal areas of the estuary along with surface samples were presented by Rollinson *et al.* (2007) along with mineralogical data based on XRD, reflected light microscopy and standard manual scanning electron microscopy. Core sample HE5 was collected from the Lelant Saltings area of the estuary (NGR SW5468 3678) on the 4th June 2001 (Figure 2). The recovered core was 91 cm in length and comprised a lower 26 cm interval of medium to coarse grained sands, overlain by 20 cm of black silty sands interlaminated with black clays, in turn overlain by 42 cm of laminated red-brown clays with thin interbedded sand beds/laminae. The uppermost 3 cm of the core is composed on a massive dark brown clay (Figure 2). Geochemical data based on bulk XRF analyses are presented in table 4 and figures 7 and 8 in Rollinson *et al.* (2007) and show that the laminated clays are extremely enriched in Sn, Cu, Zn and arsenic, with >7000 ppm Sn, >3000 ppm Cu, >2400 Zn and >1400 ppm As.

During the initial analysis of core HE5, six core plugs were extracted from the core, by gently pushing 3 cm diameter plastic tubes into the recovered core. These core plugs were slowly dried and resin-impregnated under vacuum, using a resin thinned with acetone, that aided in driving moisture from the sediment. The resin impregnated core plugs were then cut and polished. Initial work described by Rollinson *et al.* (2007) examined these resin impregnated blocks using both reflected light microscopy and also through manual scanning electron microscopy with interactive EDS analysis.

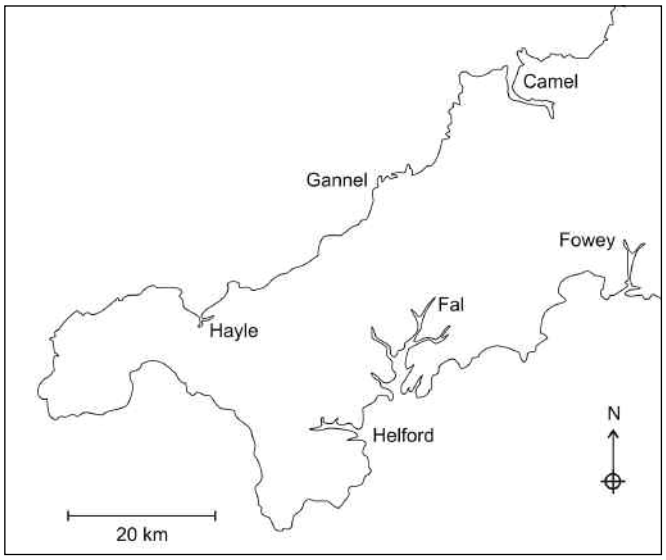

Figure 1a. *Location of the Hayle Estuary, Cornwall, UK.*

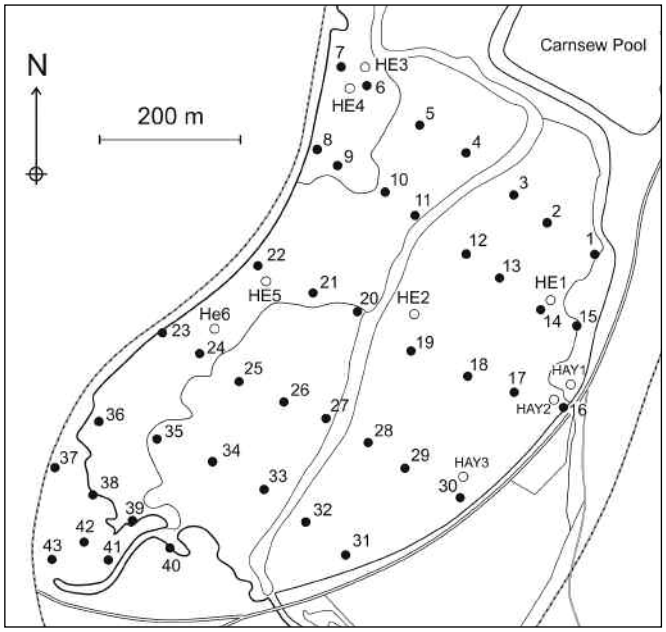

Figure 1b. *Detailed map of the western side of the estuary showing the location of core HE5 (from Rollinson* et al.*, 2007).*

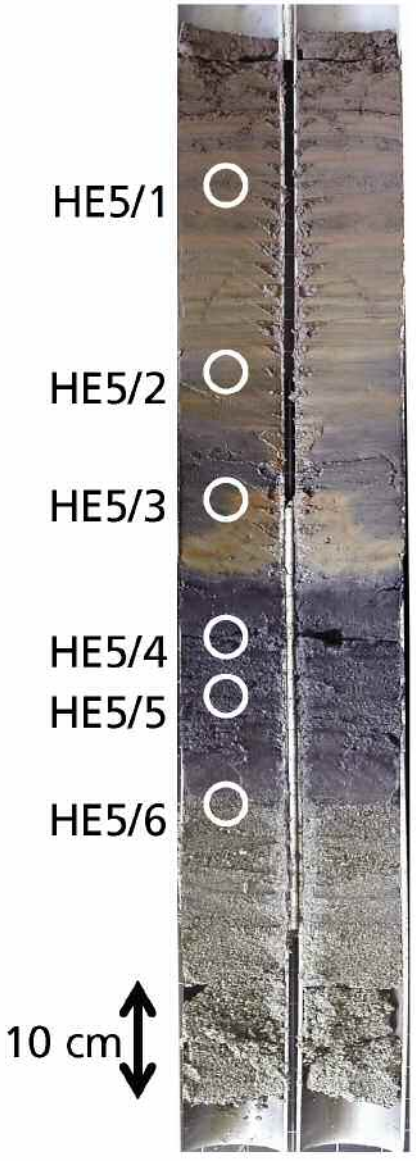

Figure 2. *Photograph showing the appearance of core HE5. The positions from which the core plugs analysed in this study are indicated.*

QEMSCAN® SAMPLE ANALYSIS AND RESULTS

In this study, the six polished blocks collected from core HE5 were re-polished, and then analysed using the QEMSCAN® system at the University of Exeter, Cornwall Campus, based on a Carl Zeiss EV50 SEM platform. In this study, the EDS detectors used were liquid nitrogen cooled SiLi detectors. QEMSCAN® automated mineral analysis can be carried out using four main different measurement modes (see Pirrie *et al.*, 2004; Pirrie *et al.*, 2009). In this study the mineralogy of the entire area of the polished blocks was measured using the fieldscan operating mode, with a 10 µm electron beam stepping interval. It can be envisaged that in this measurement mode, a 10 µm grid is superimposed over the area of the sample, and at each cross over point an ED X-Ray spectra is acquired. Each individual spectra is then assigned to a mineral or chemical grouping. In this way the entire area of the block is systematically mapped. The total number of X-Ray spectra acquired from each polished block are shown in Table 1, with between 3687016 and 4775593 discrete analysis points. Once the sample has been measured the raw data file is processed so that similar groupings are combined together to provide the final reported mineral list. The mineral categories used in this study are presented in Table 2. As well as providing the modal mineralogy, the QEMSCAN® data can be used to calculate an overall chemical assay for the analysed sample. This estimated chemical assay is based on: (a) the measured modal mineralogy and (b) the assigned mineral chemistry and density. Within the iMeasure® software, each mineral listed is assigned a chemical composition, usually the standard published formulae for that particular mineral species. The calculated chemical assay is then based upon the measured mineral

Sample Number	HE5/1	HE5/2	HE5/3	HE5/4	HE5/5	HE5/6
Depth (cm below surface)	10	28	37.5	48	58	66
No. EDS analysis points	4448603	4775593	4055470	4100178	3698715	3687016
Quartz	38.89	21.67	36.33	26.00	24.58	31.90
Calcite	0.24	0.57	7.40	9.57	27.21	20.80
CaMg(Fe) carbonates	0.02	0.03	0.08	0.07	0.04	0.05
Plagioclase	0.66	0.60	1.76	2.91	2.02	2.12
K-feldpar	22.89	38.43	17.15	20.15	16.80	16.88
Muscovite	1.17	1.40	0.83	1.13	0.68	0.81
Biotite/phlogopite/micas	0.57	1.18	0.62	0.70	0.72	0.68
Tourmaline	4.55	2.17	2.33	2.45	2.63	3.88
Clays (FeAl silicates)	22.07	26.21	24.06	25.03	18.23	15.80
MgFe silicates	1.57	1.20	1.07	0.99	0.69	0.84
CaMg(Fe) silicates	0.02	0.01	0.02	0.02	0.08	0.06
Ca(FeAl) silicates	0.11	0.15	0.57	0.88	0.78	0.78
Al silicates	0.91	0.51	1.03	0.72	0.28	0.43
Zircon	0.03	0.03	0.02	0.02	0.01	0.02
Apatite	0.37	0.27	0.17	0.17	0.10	0.12
Ca sulphates	0.01	0.02	0.22	0.35	0.28	0.15
Carbon (metal trace)	0.18	0.15	0.36	0.45	0.22	0.24
Fe-Ox/CO3	3.96	2.39	2.59	2.49	1.51	1.74
Cassiterite	0.28	0.26	0.28	0.23	0.18	0.34
Fe sulphides	0.11	0.76	0.92	2.89	1.66	0.71
CuFe sulphides	0.00	0.26	0.60	0.76	0.25	0.36
Cu sulphides	0.00	0.01	0.02	0.01	0.00	0.00
Cu Chlorides	0.00	0.01	0.02	0.02	0.00	0.00
Other Cu minerals	0.10	0.16	0.22	0.25	0.06	0.07
Zn sulphides/sulphates	0.00	0.03	0.06	0.07	0.03	0.08
Arsenopyrite	0.01	0.05	0.03	0.03	0.02	0.02
Wolframite	0.01	0.01	0.00	0.00	0.00	0.00
Ti phases	0.32	0.29	0.21	0.24	0.14	0.19
Man made phases	0.60	0.81	0.65	0.75	0.54	0.62
Monazite	0.01	0.01	0.01	0.01	0.01	0.01
Others	0.34	0.35	0.37	0.62	0.25	0.27

Table 1. *Modal mineralogy results based on QEMSCAN® automated mineral analysis.*

Mineral category	Mineral description
Quartz	Quartz and other silica minerals.
Calcite	Calcite.
CaMg (Fe) carbonates	Dolomite, ankerite, Mg rich calcite.
Plagioclase feldspars	Plagioclase feldspar.
K-feldspars	K-feldspars.
Muscovite	Muscovite.
Biotite/phlogopite/micas	Biotite, pholgopite and any other mica species.
Tourmaline	Tourmaline, including schorl.
Clays (FeAl silicates)	Chlorite, FeAl silicates.
Mg & Fe silicates	Natural and man made Fe silicates.
CaMg (Fe) silicates	May include diopside, Ca-amphiboles, hornblende, any CaMg silicate with or without iron.
Ca (Fe Al) silicates	Includes epidote, some garnets and any Ca silicate (glass?) with or without Fe & Al.
Al silicates	Kaolinite/halloysite/dickite and any other Al silicates.
Zircon	Zircon.
Apatite	Any Ca phosphate (e.g. apatite).
Ca sulphates	Gypsum.
Carbon (metal trace)	High carbon with traces of Fe, Zn, Ca, Sn, Si, Cu, As, S, Mn. May also include coal or slags.
Fe-Ox/CO3	Fe oxides and carbonates.
Cassiterite	Sn oxide, cassiterite.
Fe sulphides	Pyrite/marcasite, jarosite.
CuFe sulphides	Chalcopyrite. May include trace amounts of cubanite, bornite and other CuFe sulphides.
Cu sulphides	Cu suphides including covellite, chalcocite and diginite.
Cu minerals	Includes Cu As phases (e.g. enargite, tennantite).
Zn sulphides/sulphates	Sphalerite and any zinc sulphate
Arsenopyrite	Arsenopyrite, Fe-As-sulphides and As-sulphide phases.
Wolframite	Tungsten phases such as wolframite.
Cu chlorides	Cu chlorides such as atacamite.
Ti phases	Ilmenite, rutile and sphene/titanite, perovskite, Ti-Fe silicates.
Man made phases	Sn slags, glass, Cu slags.
Monazite	Ce phosphates, may include La, Th phosphates.
Others	Any other mineral not included above.

Table 2. *QEMSCAN® mineral categories used in this study.*

abundance and the assumed chemical formulae for the minerals present in the sample. However, it should be noted that this approach may result in the under-reporting of an elemental abundance, if that element occurs at low levels of abundance within other minerals, whose ideal formulae does not contain that element. For example arsenic and zinc may occur adsorbed on clay minerals, but would not be detected using SEM-EDS unless present at concentrations above approximately 1 wt%.

The modal mineralogy data for the six samples analysed is presented in Table 1, along with Figure 3a (gangue minerals) and Figure 3b (ore minerals). Gangue phases make up between 94 and ~98% of the modal mineralogy of the samples analysed, with ~2 to 6% total ore phases. The modal mineralogy data clearly demonstrate that calcite is abundant towards the base of the core, with a marked decrease in abundance up-core. Conversely, there is a general increase in the abundance of FeAl silicates (chlorite group clay minerals) from the base of the core towards the top of the core. There is a clear correlation between the core sedimentology and the measured mineralogy (Figure 3). The ore mineral modal abundance shows a marked change in abundance with sampling position, with ore phases present in the basal sands, increasing markedly within the dark grey silts and sands at the junction between the carbonate-rich sands below and the laminated clays above. This increase in abundance is most marked for the Fe sulphide and CuFe sulphide phases (Figure 3b). The abundance of ore minerals then decreases markedly towards the top of the core (Figure 3b). This is most marked for the sulphide phases, which might either represent a decrease in their supply, or their loss as a result of diagenetic alteration of the sediments within the oxidising upper part of the sediment profile. Core dating results presented in Rollinson *et al.* (2007) indicated that the sediments exposed at the surface of the estuary were probably deposited prior to *c.*1880, suggesting that the decrease in the abundance of sulphides in these surficial sediments may be the result of diagenetic processes rather than decreased supply of sulphide minerals to the estuary. The abundance of sulphide minerals within the dark grey silts and sands at the junction between the carbonate-rich

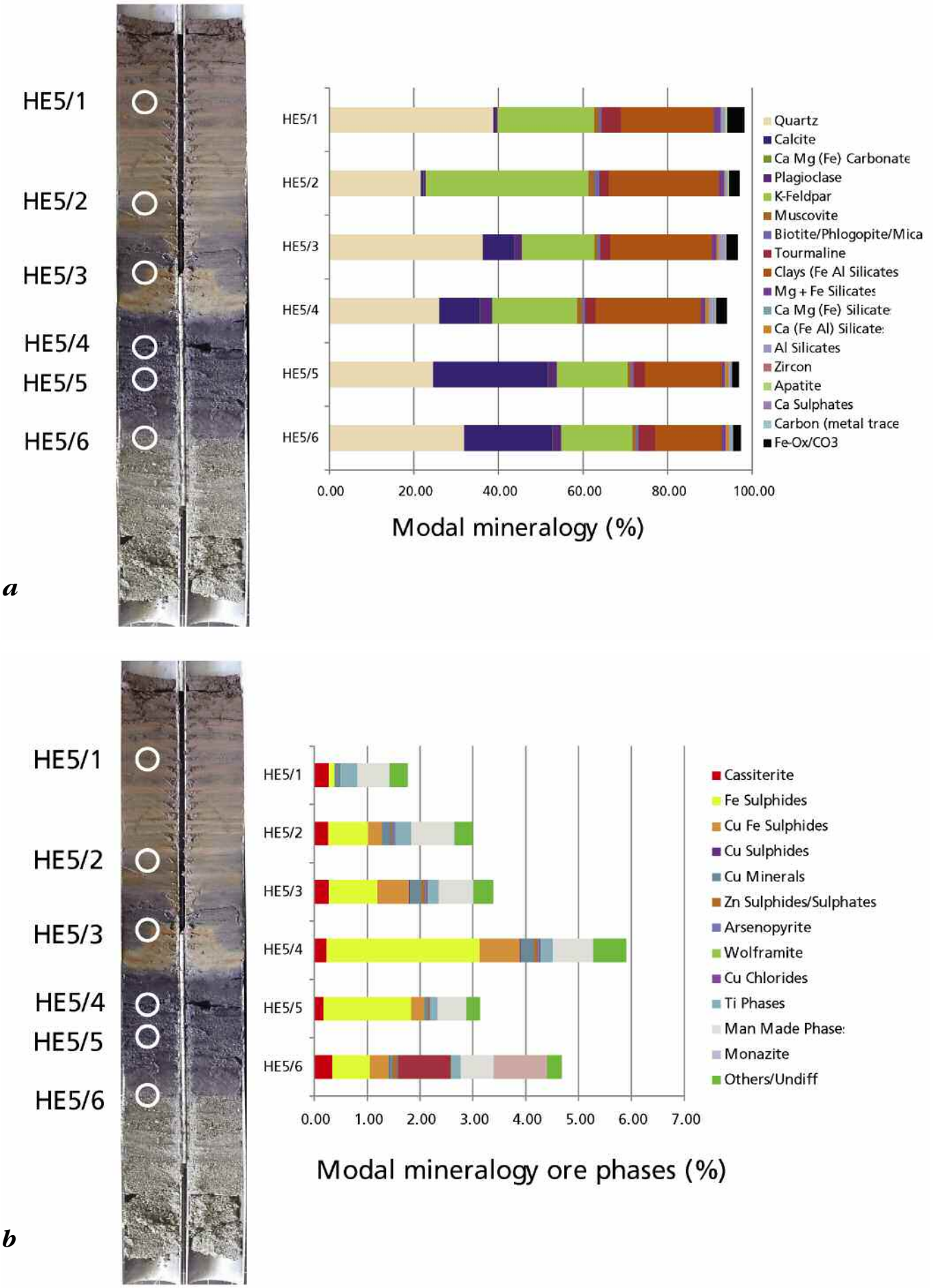

Figure 3. *QEMSCAN® modal mineralogy. (**a**) Modal mineral abundance of the gangue minerals present in the six samples analysed from core HE5. (**b**) Modal mineral abundance of the ore phases present in the six samples analysed from core HE5.*

sands below and the laminated clays above is consistent with the previous work of Pirrie *et al.* (1999) who identified a wide range of diagenetic sulphide minerals occurring at the same sedimentological setting in cores collected from the Copperhouse area of the Hayle Estaury.

The calculated QEMSCAN® assay data for As, Cu, Pb, S, Sn, W and Zn are shown graphically in Figure 4. The calculated data are also shown along with the XRF data from Rollinson *et al.* (2007) in Table 3. It should be noted that the XRF data were derived from slightly different depth intervals within the core sample than the sampling positions of the core plugs, although the closest available XRF data to the sampling positions from the core plugs are shown. The data are recalculated to fractions of percent from ppm for ease of comparison between the two data sets. There is a clear correspondence between the ore mineralogy shown in Figure 3b and the calculated geochemistry as shown in Figure 4. This is of course, in part an artefact of the data in that the calculated geochemistry is based upon the measured modal mineralogy. If the calculated and measured geochemical data are compared (Table 3) it is clear that for some elements there is a correspondence in the data, whilst for other elements there is a miss-match in the two data sets, although the overall trends with depth, are the same for all elements reported by the two different techniques. For example, the data for Sn show the closest correspondence between the actual measured (XRF) data set and the calculated

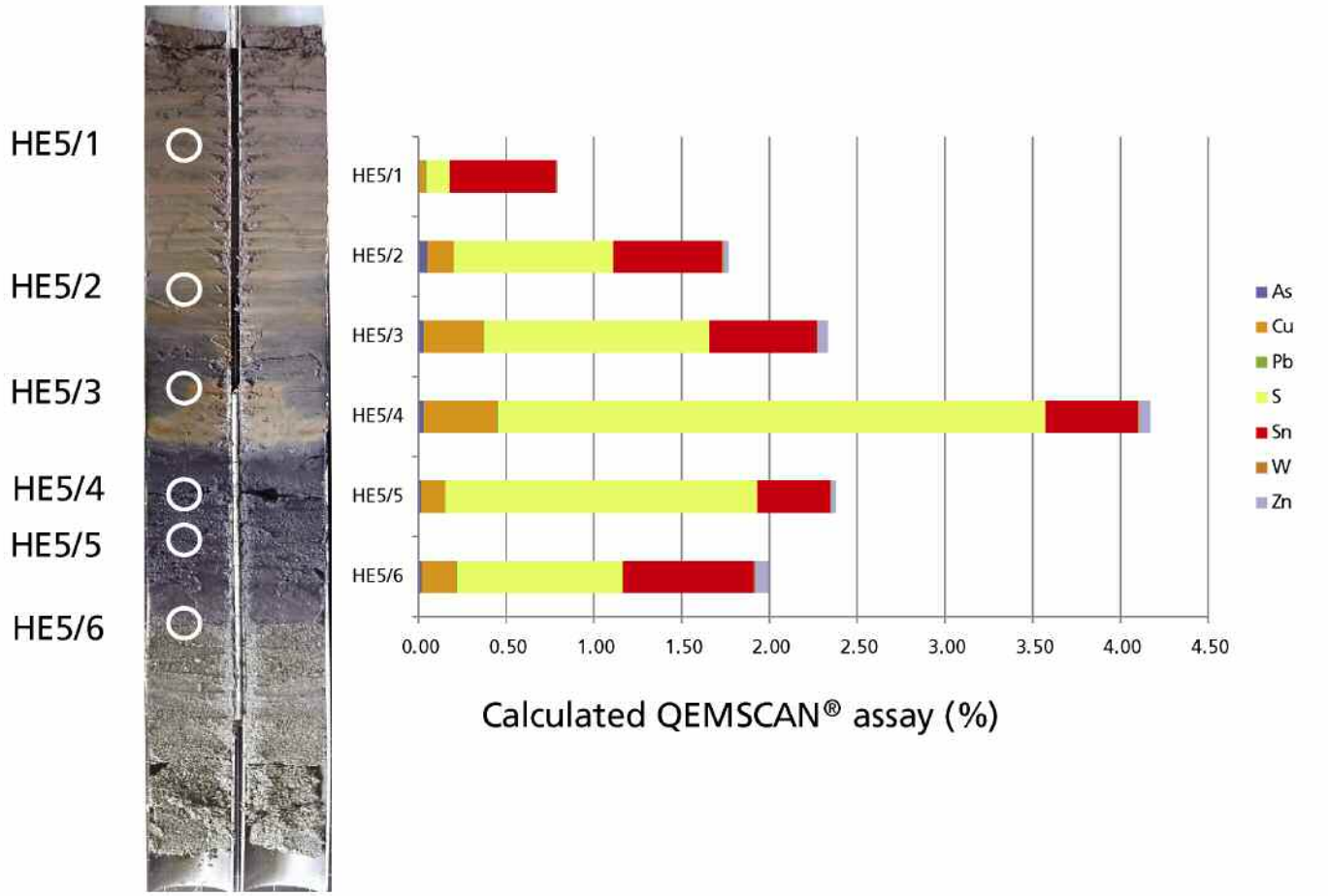

Figure 4. *Diagram showing the calculated abundance of As, Cu, Pb, S, Sn, W and Zn based on the QEMSCAN® assay.*

Polished block	HE5/1	HE5/2	HE5/3	HE5/4	HE5/5	HE5/6
Depth (cm below surface)	10	28	37.5	48	58	66
As (QEMSCAN®)	0.01	0.05	0.03	0.03	0.02	0.02
As XRF	0.07	0.14	0.09	0.08	0.05	0.03
Cu (QEMSCAN®)	0.03	0.15	0.34	0.42	0.13	0.20
Cu XRF	0.15	0.23	0.27	0.31	0.14	0.09
Pb (QEMSCAN®)	0.01	0.00	0.00	0.00	0.00	0.01
Pb XRF	0.04	0.03	0.03	0.03	0.01	0.01
Sn (QEMSCAN®)	0.60	0.62	0.61	0.53	0.41	0.75
Sn XRF	0.55	0.70	0.69	0.57	0.40	0.28
Zn (QEMSCAN®)	0.00	0.03	0.06	0.06	0.03	0.07
Zn XRF	0.08	0.11	0.20	0.24	0.13	0.09

Table 3. *Comparison of the QEMSCAN® calculated chemistry and the measured bulk chemistry based on XRF analysis.*

(QEMSCAN®) data set (Table 3) in most of the samples analysed, although there is greater variance for sample HE5/6. The greatest difference between the measured and calculated data sets is for As and Zn, with in general, the QEMSCAN® data set under-reporting the elemental abundance when compared with the XRF data set. The variance between the measured and calculated elemental data sets probably reflects the abundance of different mineralogical sites where the different elements measured may occur. For example, within this sedimentary succession the majority of the Sn is almost certainly reporting to the mineral category cassiterite, along with possibly some Sn-bearing slags. As and Zn are however, much more geochemically mobile and may be present in a much wider range of mineralogical settings within the sediments. For example, although arsenopyrite and sphalerite do occur, it is also likely that As and Zn are occurring absorbed onto clay minerals at abundances below the SEM-EDS detection level, and are not included within the calculated mineral chemistry (*cf.* Isaure *et al.*, 2005). Overall, the calculated assay data are sufficient to examine the overall elemental deportment by mineral category, but would not have sufficient accuracy or precision in a contaminated land assessment. This does not however, invalidate this methodology. For example, the calculated QEMSCAN® assay for arsenic indicates what proportion of the arsenic present is occurring in specific arsenic-bearing minerals.

During the analysis of the polished blocks, a false colour composite image of the samples is created. These are shown in Figure 5. Each image is a false colour 'map' showing the distribution of the different mineralogical groupings or chemical groupings within the QEMSCAN® processed mineral list. The lamination within the upper part of the core is clearly defined by both grain size and mineralogical variation (Figure 5) and the core plug recovery technique and sample preparation methodology has clearly not significantly disrupted the laminated sediments. It is interesting to note that the upper laminated interval of the core displays very fine parallel lamination implying very little bioturbation. The lower, more sand dominated intervals are more 'disturbed' either as a function of core/sediment plug recovery, or possibly as a result of increased levels of bioturbation in the lower intervals of the core.

Discussion

Whilst automated SEM-EDS analysis is widely used within the global mining industry, it has yet to be universally adopted within other areas of the earth and environmental sciences. This is probably because up until the last few years, there were very few published papers documenting the analytical capability of modern automated SEM-EDS analytical systems. Many historical mine sites world-wide are contaminated as a result of the release of tailings and mineral processing waste streams (e.g. Bosso *et al.*, 2008; Göktepe, 2005; Power *et al.*, 2009) and at such sites understanding the mineralogy/phase composition of the particulate waste is necessary in the assessment of the risk posed to health. In addition, an

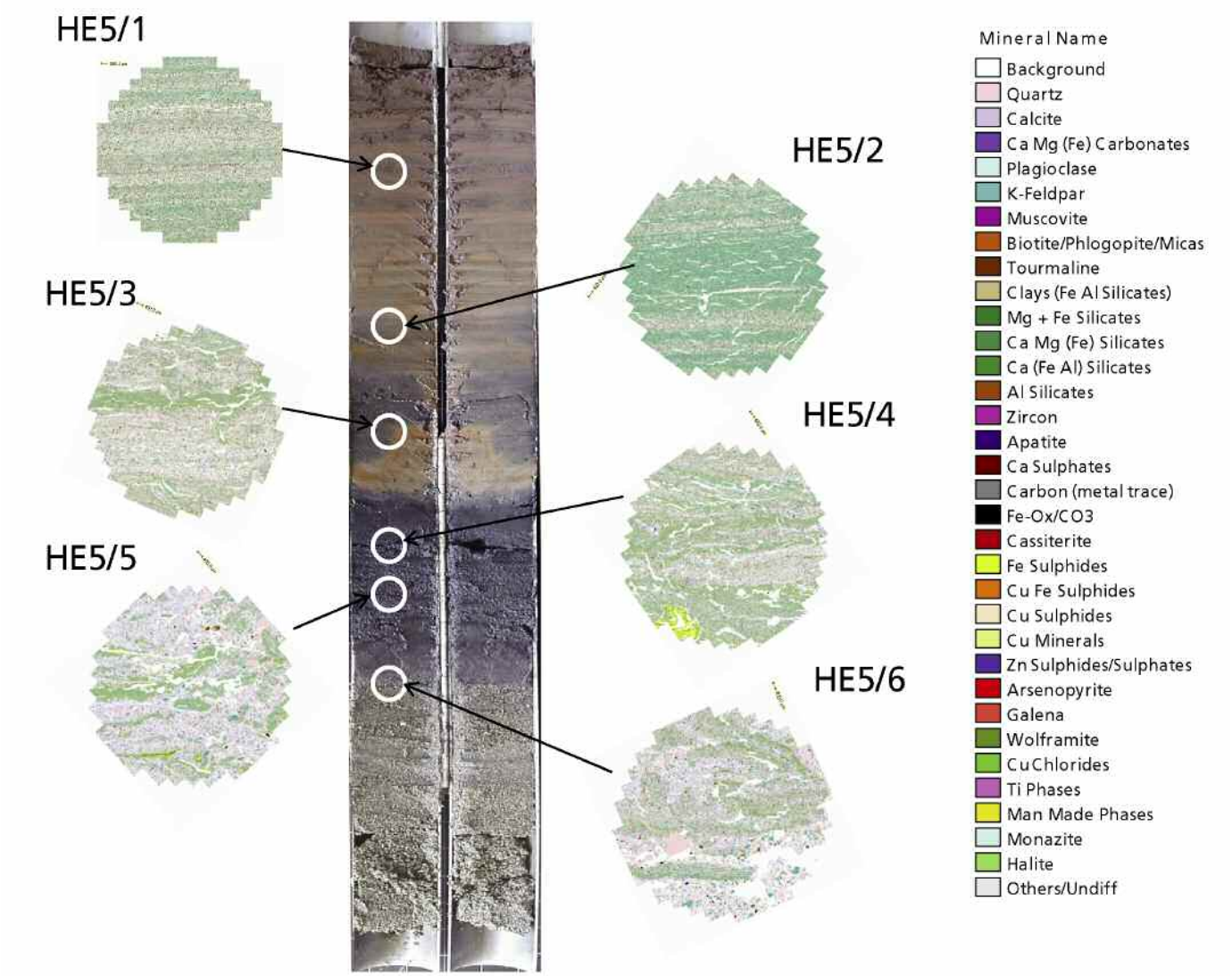

Figure 5. *QEMSCAN® fieldscan images of the analysed samples from core HE5.*

understanding of the mineralogy of the waste streams is directly relevant when different soil remediation strategies are being considered (e.g. Cundy *et al.*, 2008; Göktepe, 2005). The advantages of automated SEM-EDS analysis are that very large numbers of particles can be analysed, providing statistically robust data sets. In addition, during routine sample measurement, textural and particle size data are also automatically collected which may be significant in the interpretation of the origin of the phase, as well as aiding the design of a remediation strategy. The measurement parameters can be tailored to the specific investigation; for example, in this study the electron beam stepping interval was set at 10 µm; a higher resolution beam stepping interval of 1 µm may have identified many more ore phases in the sub 10 µm grain size fraction. In addition, mineralogical data can be used in an environmental forensic assessment of the possible sources of a contaminant phase.

The main limitations to automated SEM-EDS analysis of contaminated soils/sediments are that: (1) typically only inorganic phases can be characterised, although it should be noted that particles of coal etc can be measured; (2) whilst detection limits of discrete minerals are very good, the detection of metals absorbed or adsorbed onto other mineral surfaces etc may not be possible, unless the contaminant element is present at concentrations above approximately 1 wt%; (3) increasingly, environmental legislation is reducing the absolute concentration of an element in a soil or sediment that is allowable before remediation is required; the detection limits for automated mineral analysis are too high for such low level determinations. However, where wastes are present as particulate inorganic grains, automated mineral analysis can provide valuable data sets.

Acknowledgements

Fieldwork in the Hayle Estuary was allowed by kind permission of the local RSPB reserve manager Dave Flumm. The preparation of the resin plugs analysed was carried out by Stephen Pendray. XRF analysis was assisted by Fiona Thomas. We are grateful to Alan Butcher, Alastair Ruffell and Andy Cundy for their reviews of the draft manuscript, and to Robin Shail for editorial comments.

References

ANDERSON, J.C.O., ROLLINSON, G.K., SNOOK, B., HERRINGTON, R. and FAIRHURST, R.J. 2009. Use of QEMSCAN® for the characterisation of Ni-rich and Ni-poor goethite in laterite ores. *Minerals Engineering*, **22**, 1119-1129.

BENEDICTUS, A., BERENDSEN, P. and HAGNI, A.M. 2008. Quantitative characterisation of processed phlogopite ore from Silver City Dome District, Kansas, USA, by automated mineralogy. *Minerals Engineering*, **21**, 1083-1093.

BOSSO, S.T., ENZWEILLER, J. and ANGELICA, R.S. 2008. Lead bioaccessibility in soil and mine wastes after immobilization with phosphate. *Water, Air and Soil Pollution*, **195**, 257-273.

CAMM, G.S., BUTCHER, A.R., PIRRIE, D., HUGHES, P.K. and GLASS, H.J. 2003. Secondary mineral phases associated with a historic arsenic calciner identified using automated scanning electron microscopy; a pilot study from Cornwall, U.K. *Minerals Engineering*, **16**, 1269-1277.

CUNDY, A.B., HOPKINSON, L. and WHITBY, R.L.D. 2008. Use of iron-based technologies in contaminated land and groundwater remediation: A review. *Science of the Total Environment*, **400**, 42-51.

ENVIRONMENT AGENCY. 2009. Soil guideline values for inorganic arsenic in soil. *Science Report SC050021/arsenic* SGV.

GÖKTEPE, F. 2005. Treatment of lead mine waste by a Mozley multi-gravity separator (MGS). *Journal of Environmental Management*, **76**, 277-281.

HARDY, A.D. and ROLLINSON, G.K. 2009. Green eye cosmetics of antiquity. *Pharmaceutical Historian*, **39**, 2-7.

HARDY, A.D., WALTON, R.I., VAISHNAV, R., MYERS, K.A., POWER, M.R. and PIRRIE, D. 2006. Egyptian eye cosmetics ('kohls'): past and present. In: BRADLEY, D. and CREAGH, D. (Eds), *Physical techniques in the study of art, archaeology and cultural heritage*. Elsevier, 173-203.

INTAWONGSE, M. and DEAN, J.R. 2008. Use of the physiologically-based extraction test to assess the oral bioaccessibility of metals in vegetable plants grown in contaminated soil. *Environmental Pollution*, **152**, 60-72.

ISAURE, M.P., MANCEAU, A., GEOFFROY, N., LABOUDIGUE, A., TAMURA, N. and MARCUS, M.A. 2005. Zinc mobility and speciation in soil covered by contaminated dredged sediment using micrometer-scale and bulk averaging X-ray fluorescence, absorption and diffraction techniques. *Geochemica et Cosmochimica Acta*, **69**, 1173-1198.

LUO, Q., CATNEY, P. and LERNER, D. 2009. Risk-based management of contaminated land in the UK: Lessons for China ? *Journal of Environmental Management*, **90**, 1123-1134.

MARTIN, R.S., MATHER, T.A., PYLE, D.M., POWER, M., ALLEN, A.G., AIUPPA, A., HORWELL, C.J. and WARD, E.P.W. 2008. Composition-resolved size distribution of volcanic aerosols in the Mt. Etna plumes. *Journal of Geophysical Research*, **113**.

NEL., P., LAU, D., HAY, D. and WRIGHT, N. 2006. Non-destructive micro X-ray diffraction analysis of painted artefacts: Determination of detection limits for the chromium oxide-zinc oxide matrix. *Nuclear Instruments and Methods in Physics Research*, **B251**, 489-495.

PASCOE, R.D., POWER, M.R. and SIMPSON, B. 2007. QEMSCAN analysis as a tool for improved understanding of gravity separator performance. *Minerals Engineering*, **20**, 487-495.

PIRRIE, D., BEER, A.J. and CAMM, G.S. 1999. Early diagenetic sulphide minerals in the Hayle Estuary, Cornwall. *Geoscience in south west England*, **9**, 325-332.

PIRRIE, D., POWER, M.R., ROLLINSON, G., CAMM, G.S. and HUGHES, S.H. 2003. The spatial distribution and source of arsenic, copper, tin and zinc within the surface sediments of the Fal Estuary, Cornwall, UK. *Sedimentology*, **50**, 579-595.

PIRRIE, D., BUTCHER, A.R., POWER, M.R., GOTTLIEB, P. and MILLER, G.L. 2004. Rapid quantitative mineral and phase analysis using automated scanning electron microscopy (QemSCAN); potential applications in forensic geoscience. In: PYE, K. & CROFT, D. (Eds), *Forensic Geoscience*. Geological Society, London, Special Publication, **232**, 123-136.

PIRRIE, D., POWER, M.R., ROLLINSON, G.K., WILTSHIRE, P.E.J., NEWBERRY, J. and CAMPBELL, H.E. 2009. Automated SEM-EDS (QEMSCAN®) mineral analysis in forensic soil investigations; testing instrumental variability. In: RITZ, K., DAWSON, L. and MILLER, D. (Eds), *Criminal and Environmental Soil Forensics*. Springer, 411-430.

POWER, M.R., PIRRIE, D., CAMM, G.S. and ANDERSEN, J.C.O. 2009. The mineralogy of efflorescence on arsenic calciner buildings in SW England. *Mineralogical Magazine*, **73**, 27-42.

ROLLINSON, G.K., PIRRIE, D., POWER, M.R., CUNDY, A and CAMM, G.S. 2007. Geochemical and mineralogical record of historical mining, Hayle Estuary, Cornwall, UK. *Geoscience in south-west England*, **11**, 326-337.

ROSADO, L., MORAIS, C., CANDEIAS, E.A., PINTO, A.P., GUIMARAES, F. and MIRAO, J. 2008. Weathering of S. Domingos (Iberian Pyrite Belt) abandoned mine slags. *Mineralogical Magazine*, **72**, 489-494.